MODELING OF MULTIPATH FADING CHANNELS FOR NETWORK SIMULATION

A Thesis

by

RAJKUMAR SAMUEL

Submitted to the Office of Graduate Studies of
Texas A&M University
in partial fulfillment of the requirements for the degree of

MASTER OF SCIENCE

May 2007

Major Subject: Electrical Engineering

MODELING OF MULTIPATH FADING CHANNELS FOR NETWORK SIMULATION

A Thesis

by

RAJKUMAR SAMUEL

Submitted to the Office of Graduate Studies of
Texas A&M University
in partial fulfillment of the requirements for the degree of

MASTER OF SCIENCE

Approved by:

Chair of Committee,	Scott L. Miller
Committee Members,	Don R. Halverson
	A. L. Narasimha Reddy
	Jennifer L. Welch
Head of Department,	Costas N. Georghiades

May 2007

Major Subject: Electrical Engineering

ABSTRACT

Modeling of Multipath Fading Channels
for Network Simulation. (May 2007)
Rajkumar Samuel, B.E., Anna University, India
Chair of Advisory Committee: Dr. Scott L. Miller

Development of accurate physical layer models is very important for generating realistic network simulation results. Significant effort has been put into setting up physical layer models for wireless channels that emulate the impact of the channel on the higher layers of the network. Setting up the models is especially difficult for a frequency selective channel. In this thesis the use of non-linear functions to convert the frequency selective channel to an equivalent flat fading channel is examined. The analytical expressions for the statistics of the equivalent flat fading process that are needed to set up the physical layer models are derived. These results are used to set up the physical layer model for the frequency selective channel. Extensive simulations are performed to verify the accuracy of the model against a detailed physical layer implementation. The statistics of the model and the actual channel are seen to match, validating the method of setting up the models.

To Thatha and Aachi.

ACKNOWLEDGMENTS

I would like to thank my advisor Dr. Scott Miller for his guidance and support in completing this thesis and throughout my degree program. I would also like to thank my committee members Dr. Don Halverson, Dr. Narasimha Reddy and Dr. Jennifer Welch for reviewing and helping improve this thesis with their suggestions. I thank the department of Electrical and Computer Engineering and the Department Head Dr. Costas Georghiades for providing the opportunity and the resources to complete this work. A special thank you to Yi for all the invaluable assistance and the time invested in the fruitful discussions.

I thank my parents and grand parents back home for their support and my family here, especially Vinod and Kaivtha for their love and care. I would like to thank Aarthi and all my friends and roommates at College Station for a great time filled with wonderful memories.

TABLE OF CONTENTS

CHAPTER Page

LIST OF TABLES

LIST OF FIGURES

FIGURE Page

CHAPTER I

INTRODUCTION

The prospect of having broadband Internet access over a wireless wide area network is fast becoming a reality. It is projected as a solution to the last mile bottleneck that affects conventional wireline data networks [1]. Besides being able to provide connectivity to fixed users as is available now wireless Wide Area Networks create the possibility of delivering high speed connections to mobile users as well [2].

Delivering data over wireless networks is a lot more challenging than over wireline networks. This is due to the impairments inherent in the wireless channel. Phenomenon such as fading can lead to a large number of packet drops that are not common in the wired scenario. This is particularly significant as the behavior of the physical layer can drastically affect the performance of higher level protocols and ultimately the applications that run on them. A classic example of this would be what happens to a TCP flow over a wireless link where packets are dropped. TCP assumes that packets are dropped solely due to network congestion [3] and in an effort to avoid overloading an already congested network reduces the transmission rate everytime it detects a packet loss. Thus it would lead to very poor utilization of the network resources if the protocols are designed oblivious to the lossy nature of the underlying medium.

Most applications and protocols in use today were assume a relatively reliable wired physical channel and hence when they are ported to a wireless environment it is essential to determine if they will still behave as expected. This is usually done by extensive simulation but for these results to have any correlation to what could

---

The journal model is *IEEE Transactions on Automatic Control*.

be expected in the field the models need to accurately characterize the behavior of the channel. On the other hand a complex model that precisely portrays the channel but makes it impossible to get results in a reasonable amount of time in simulations involving large networks is of no practical use. Therefore simple models that accurately abstract the essence of the channel's nature and at the same time do not drastically increase the run time are needed.

Over the years a large number of models of varying complexity and accuracy have been proposed especially for the flat faded Rayleigh channel. However when it comes to broadband wireless networks and especially those deployed in urban areas the system bandwidth is much larger than the channel coherence bandwidth and the channel is frequency selective. A novel approach to describe both flat and frequency selective channels with a simple Four State Markov Model(4SMM) is presented in [4]. The 4SMM has low complexity and at the same time provides a close match to the results that are obtained by a full detailed physical layer with explicit modulation, coding and fading channel modeling. The analytical approach to setting up the models for the flat and frequency selective channel is presented and this makes it possible to set up the models without presimulation. However in the case of a frequency selective channel it is necessary to estimate the diversity order actually achieved by the particular modulation coding scheme at the SNR of interest to set up the model. There is no direct way of getting this parameter except for the asymptotic cases and simulation is required. In this thesis we explore the use of non-linear functions to convert the frequency selective channel into an equivalent flat faded channel thereby enabling the use of the models designed for use with a flat fading channel. In particular we show that the use of the mapping from a frequency selective channel to a flat channel provided by the Effective Exponential SNR Mapping(EESM) in conjunction with the 4SMM provides promising results.

The remainder of this thesis is structured as follows. Chapter II describes the wireless channel model. Chapter III explains the EESM function and the approach to get the parameters of the function for various modulation and coding schemes. In Chapter IV we present the setting up of the 4SMM model for a frequency selective channel by using the EESM function to convert it to an equivalent flat fading channel. It also contains a comparison of the frame error statistics of the model and the full physical layer. Chapter V concludes the thesis.

CHAPTER II

BACKGROUND ON FADING MODELS

The biggest challenge posed by the wireless channel is the small scale fading cause by the presence of multiple paths between the transmitter and receiver. It is this phenomenon that causes rapid changes in the signal strength over small distances or time and contributes to packets getting dropped. In this chapter we present the statistical models for the fading in a wireless channel. The method of generating a fading channel is also presented.

A. Multipath Fading

In a wireless environment there are several paths that a signal can take between the transmitter and receiver. These paths can add constructively or destructively depending on the phase of the different signal paths at a given point. As the phase changes by 2π over one wavelength the received signal power changes very rapidly with distance. When the channel or the terminals are in motion this fluctuation over distance manifests itself as rapid fluctuations of the signal strength in time.

Fading is classified based on the relationship between the signal parameters and the channel parameters. The coherence time of a channel is a measure of how quickly the channel response decorrelates. When the symbol duration is small compared to the coherence time the fading is termed as slow fading. When the symbol duration is comparable to the coherence time of the channel the fading is termed fast. Another classification of the fading process depends on the relationship between the delay spread of the channel which is a measure of its time dispersiveness and the symbol duration. When the delay spread is much smaller than the symbol duration the fading is classified as flat and when it is not it is termed as frequency selective fading.

1. Flat Fading

The equivalent complex baseband received signal $r(t)$ in a multipath channel can be expressed as

$$r(t) = \sum_{k=1}^{N} \alpha_k(t) e^{j\theta_k(t)} s(t - \tau_k) + n(t) \tag{2.1}$$

where α_k, θ_k and τ_k are the multiplicative gain, phase shift and the delay of the k^{th} path, N is the total number of paths $s(t)$ is the transmitted signal and $n(t)$ is the Additive White Gaussian Noise term.

When the path delays are small compared compared to the symbol duration $s(t - \tau_k) \approx s(t)$ and the received signal can be expressed as

$$\begin{aligned} r(t) &= \sum_{k=1}^{N} \alpha_k(t) e^{j\theta_k(t)} s(t) + n(t) \\ &= g(t)s(t) + n(t) \end{aligned} \tag{2.2}$$

where

$$g(t) = x(t) + jy(t) \tag{2.3}$$

$$x(t) = \sum_{k=1}^{N} \alpha_k(t) \cos\theta_k(t) \tag{2.4}$$

$$y(t) = \sum_{k=1}^{N} \alpha_k(t) \sin\theta_k(t) \tag{2.5}$$

From the above equation we can see that the original transmitted signal is modulated by a random time varying scale factor $g(t)$. $x(t)$ is the in-phase component and $y(t)$ is the quadrature component of the gain. When the number of paths is large we can use the Central Limit Theorem to show that $x(t)$ and $y(t)$ are independent Gaussian random processes. This type of fading is known as Rayleigh fading as the envelope of the scale factor $|g(t)|$ follows a Rayleigh distribution shown in Figure 1.

$$f_R(r) = \frac{r}{\sigma^2} e^{-\frac{r^2}{2\sigma^2}}, r \geq 0 \tag{2.6}$$

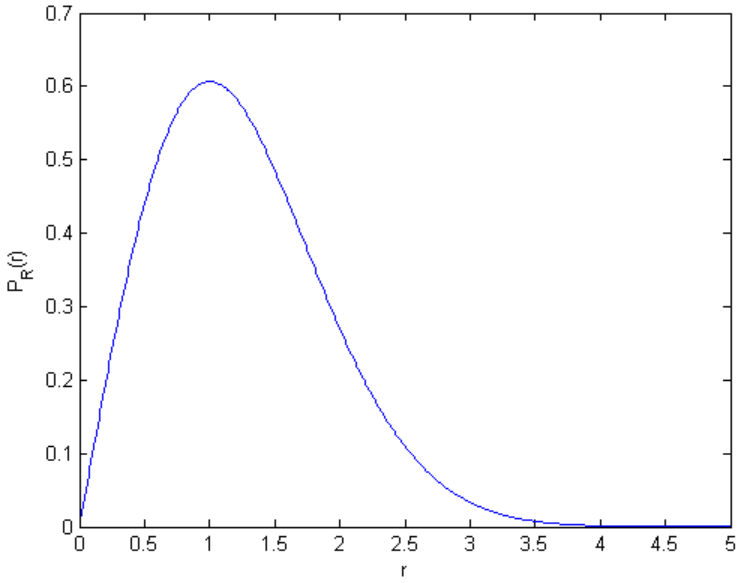

Fig. 1. PDF of Rayleigh Fading Envelope

The phases θ_k are uniformly distributed in the interval $[0, 2\pi]$ and independent for each path. This type of fading is the most commonly dealt with type of fading in the literature and is a good model for urban areas where there is no dominant or line-of-sight path available between the transmitter and the receiver.

Let Ω_p be the total power in all the paths i.e. $\Omega_p = E[x^2(t)] + E[y^2(t)] = \sum_{k=1}^{N} \alpha_k^2$ and f_m is the Doppler rate of the channel. Then it can be shown that the crosscorrelation between the in-phase and quadrature components is

$$\begin{aligned} R_{XY}(\tau) &= E_\theta[x(t)y(t+\tau)] \\ &= \frac{\Omega_p}{2} E_\theta[\sin(2\pi f_m \tau \cos(\theta))] \\ &= 0 \end{aligned} \tag{2.7}$$

Thus the in-phase and quadrature components are uncorrelated and therefore independent Gaussian random processes. The autocorrelation of $x(t)$ and $y(t)$ is

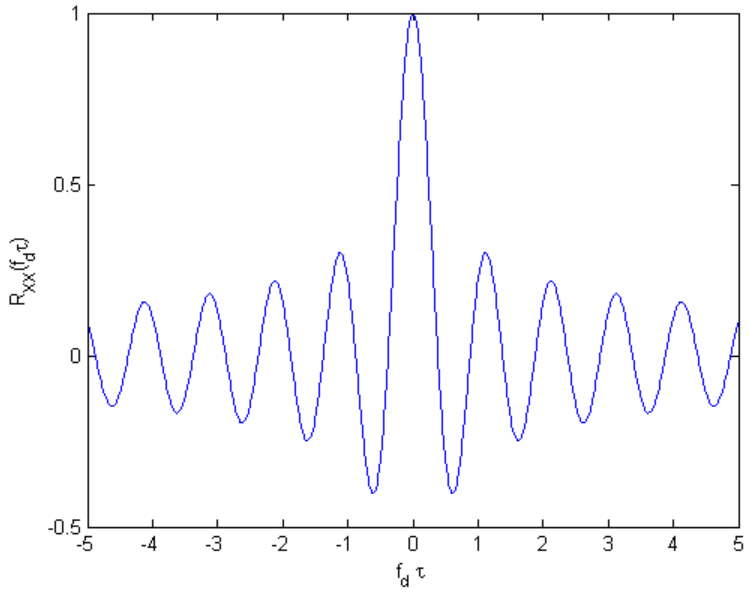

Fig. 2. Autocorrelation of In-Phase and Quadrature-Phase Terms of Rayleigh Fading

given by

$$\begin{aligned} R_{XX}(\tau) &= E_\theta[x(t)x(t+\tau)] \\ &= \frac{\Omega_p}{2} E_\theta[\sin(2\pi f_m \tau \cos(\theta))] \\ &= \frac{\Omega_p}{2} J_0(2\pi f_m \tau) \end{aligned} \tag{2.8}$$

where J_0 is the zero-order Bessel function of the first kind shown in Figure 2.

The power spectral density shown in Figure 3 is obtained from the autocorrelation function by the Fourier transform.

$$\begin{aligned} S_{XX}(f) &= F[R_{XX}(\tau)] \\ &= \frac{\Omega_p}{2\pi f_m} \frac{1}{\sqrt{1-(\frac{f}{f_m})^2}}, |f| < f_m \end{aligned} \tag{2.9}$$

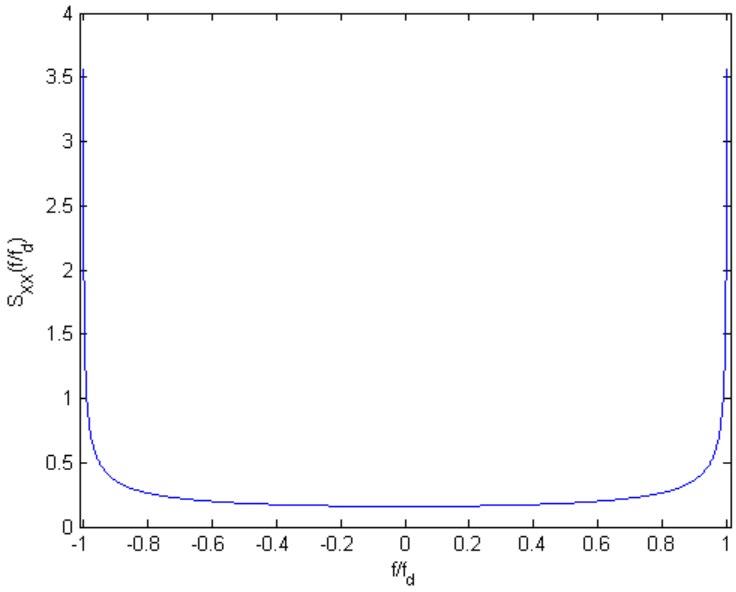

Fig. 3. Doppler Spectrum

2. Frequency Selective Fading

Only when the symbol duration is much larger than the delay spread of the channel can the fading be considered to be flat. In the frequency domain this is equivalent to the coherence bandwidth of the channel which is inversely related to the delay spread being larger than the bandwidth occupied by the signal. In this case the channel phase and magnitude response is the same across the signal bandwidth. However for high datarate applications the signal bandwidth increases and the symbol period is on the order of a few microseconds. The delay spread for urban areas ranges between 1-30 microseconds [5]. Now the channel can no longer be considered a flat fading channel and the phase and magnitude response of the fading channel is a function of frequency as well as time.

The frequency selective fading channel can be modeled as an L tap filter shown in Figure 4. L is the number of resolvable paths provided by the channel and is a

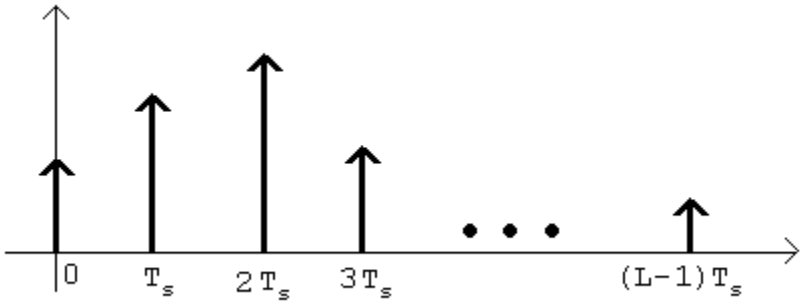

Fig. 4. L Tap Channel Model

measure of the diversity available in the channel.

$$L = \left\lfloor \frac{T_d}{T_s} \right\rfloor + 1 \tag{2.10}$$

where T_d is the delay spread of the channel and T_s is the symbol duration. The impulse response of the channel can be then expressed as

$$h(\tau, t) = \sum_{k=1}^{L} h_k(t)\delta(\tau - kT_s) \tag{2.11}$$

The usual model assumed for frequency selective fading is Wide Sense Stationary with Uncorrelated Scattering (WSSUS). This implies that the tap gains are uncorrelated. Each tap undergoes flat fading with autocorrelation of the in-phase and quadrature components being the zero-order Bessel function of the first type.

$$R_{X_k X_k} = \frac{\Omega_k}{2} J_0(2\pi f_m \tau) \tag{2.12}$$

where Ω_k is the power in each tap and the total power in all the taps adds up to Ω_p

B. Frequency Diversity

Frequency selective channels present opportunities as well as problems. The delay spread in the channel being comparable or larger than a symbol period causes Inter Symbol Interference (ISI) and additional complexity in the signal processing is required at the receiver. On the other hand because the resolvable paths are independent it is unlikely that all of them will be in a deep fade simultaneously. If the receiver is somehow able to exploit this availability of independent signal paths and utilize the frequency diversity in the channel it could provide a much more reliable system than what could be achieved in a flat fading channel without frequency diversity at the same average signal to noise ratio. This gain is called the diversity gain achieved by the system and can be measured by the negative slope of the error probability curve when both the error probability and the signal to noise ratio are in a logarithmic scale of the same base [6]. There are three common approaches to extract frequency diversity and mitigate ISI on the frequency selective channel. They are

- Single Carrier with Equalization
- Direct-sequence Spread-Spectrum
- Multi-carrier Systems

Orthogonal Frequency Division Multiplexing(OFDM) is a discrete implementation of the Multi-carrier modulation. In OFDM the wideband channel is divided into a number of smaller orthogonal subchannels. The width of the subchannels is less than the coherence bandwidth of the channel and hence they are essentially flat. Appropriate interleaving and coding across the subchannels enables the system to extract the frequency diversity of the channel. OFDM has emerged as the technology of choice in a large number of standards for high speed wireless data networks. The

802.11a and 802.11g for indoor wireless LANs and the emerging 802.16 (WiMAX) standards for mobile and fixed wide area wireless networks are some of the standards that use OFDM. In this thesis the simulation results are presented for data networks that run on an OFDM based physical layer. We use the 802.11a standard specifications for the implementation.

C. Orthogonal Frequency Division Multiplexing

OFDM uses the idea that sinusoids are eigen functions of a linear time-invariant(LTI) channel implying that when a sinusoid is input to an LTI system the output is the same sinusoid with a complex scaling factor. So signaling with a set of orthogonal sinusoids over such a channel can lead to a simple demodulator design at the receiver. This is the principle on which OFDM is based where it is assumed that fading is slow enough that the channel can be considered to be time-invariant over the signaling period. However the sinusoids have an infinite duration and when the signaling is over a finite duration say N symbols it is no longer an eigen function. The eigen function property can be achieved for finite duration signaling by the addition of a cyclic prefix to the beginning of the N symbol block. The cyclic prefix for an L tap channel is the last $L-1$ symbols of the N symbol block. The $N+L-1$ block of symbols form the OFDM symbol. The cyclic prefix is discarded at the receiver side and only the N original symbols are processed. This eliminates the ISI between two OFDM symbols as the channel impulse response lasts for only L symbol periods and the ISI from the previous OFDM symbol only affects the cyclic prefix of the current OFDM symbol. The OFDM architecture is illustrated in Figure 5.

A matrix formulation for the OFDM system is presented below. Let X be the

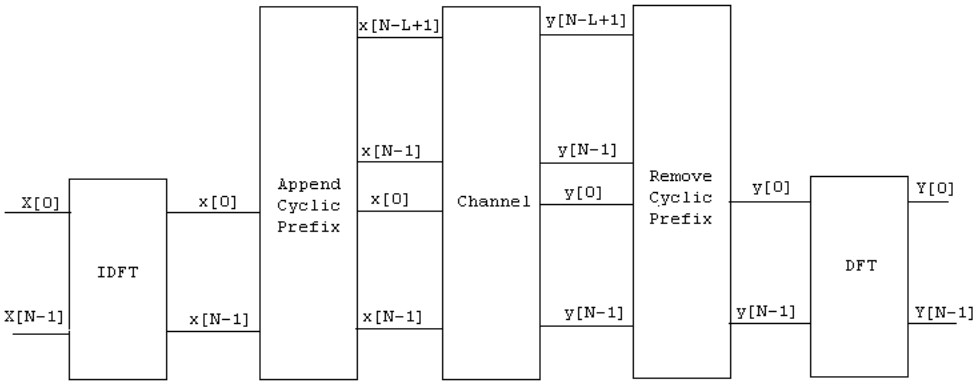

Fig. 5. OFDM Transmitter and Receiver

N symbol data sequence.

$$x = IDFT(X) \tag{2.13}$$

The cyclic prefix taken from the last $L-1$ symbols of x followed by the N symbol sequence x is transmitted over the L tap channel with impulse response $h(n)$

$$h(n) = \sum_{k=0}^{L-1} h(k)\delta(n-k) \tag{2.14}$$

The impulse response is assumed to be time invariant over an OFDM symbol block. Let y be the received vector after discarding the ISI corrupted cyclic prefix. Y is the received data sequence given by $Y = DFT(y)$.

The DFT and the IDFT function are defined as

$$DFT\{x[n]\} = \sum_{n=0}^{N-1} x[n]e^{-\frac{j2\pi kn}{N}}, k = 0, 1 \ldots N-1 \tag{2.15}$$

$$IDFT\{X[n]\} = \sum_{k=0}^{N-1} X[k]e^{\frac{j2\pi kn}{N}}, n = 0, 1 \ldots N-1 \tag{2.16}$$

In matrix form the DFT and the IDFT can be written as

$$X = Qx \tag{2.17}$$

$$x = Q^H x \tag{2.18}$$

where Q is a unitary matrix of the form with $W_N = e^{-\frac{j2\pi}{N}}$

$$Q = \frac{1}{\sqrt{N}} \begin{bmatrix} 1 & 1 & 1 & \dots & 1 \\ 1 & W_N & W_N^2 & \dots & W_N^{N-1} \\ \vdots & \vdots & \ddots & \vdots & \vdots \\ 1 & W_N^{N-1} & W_N^{2(N-1)} & \dots & W_N^{(N-1)^2} \end{bmatrix} \tag{2.19}$$

Due to the presence of the cyclic prefix the received vector y can be expressed as

$$y = Hx + v \tag{2.20}$$

where v is the complex Gaussian noise vector and H is a circulant matrix given by

$$H = \begin{bmatrix} h_0 & h_1 & \dots & h_{L-1} & 0 & \dots & 0 \\ 0 & h_0 & \dots & h_{L-2} & h_{L-1} & \dots & 0 \\ \vdots & \vdots & \ddots & \ddots & \ddots & \ddots & \vdots \\ 0 & \dots & 0 & h_0 & \dots & h_{L-2} & h_L \\ \vdots & \vdots & \ddots & \ddots & \ddots & \ddots & \vdots \\ h_2 & h_3 & \dots & 0 & \dots & h_0 & h_1 \\ h_1 & h_2 & \dots & 0 & \dots & 0 & h_0 \end{bmatrix} \tag{2.21}$$

It can be shown that the eigen vectors of a circulant matrix are the rows of the DFT matrix which implies that $H = Q^H \Lambda Q$. Λ is a diagonal matrix with its diagonal elements being the eigen values of matrix H.

$$\Lambda = Diag([\lambda_1, \lambda_1 \dots \lambda_N]) \tag{2.22}$$

$$\lambda_i = \sum_{k=0}^{L-1} h(k) e^{-\frac{j2\pi ki}{N}} \tag{2.23}$$

The received data sequence can then be written as

$$\begin{aligned} Y &= Qy \\ &= Q(Hx + v) \\ &= QHQ^H X + Qv \\ &= QQ^H \Lambda Q Q^H X + \tilde{v} \\ &= \Lambda X + \tilde{v} \end{aligned} \tag{2.24}$$

$\tilde{v}$ is only a rotation of the original complex Gaussian vector and hence it has the same statistics. Thus OFDM breaks down the frequency selective channel into N parallel non interfering flat fading channels.

$$Y_i = \lambda_i X_i + \tilde{v}_i, i = 0, 1 \ldots N-1 \tag{2.25}$$

D. Fading Process Generation

To accurately model the fading process in a link level simulation a method of generating the coefficients of the channel impulse response as a function of time is needed. There are three popular methods of generating a flat fading Rayleigh process. They are

- Sum of sinusoids or Jakes method
- IDFT Method
- Filtering White Gaussian Noise

A comprehensive survey of these methods is provided in [7]. The filtering method is the best compromise between accuracy and memory requirements. The input is a white complex Gaussian sequence and the filter output is also complex Gaussian

but with the appropriate correlation between the samples. The filter coefficients are chosen so as to match the required autocorrelation function (zero-order Bessel function of the first kind) or equivalently the bathtub shaped power spectral density. There are several ways of designing the filter. One method is to use a third order filter [8] to generate the Rayleigh fading process.

The third order filter has analog frequency response $H_3(s)$ and is implemented as the cascade of a first oder filter $H_1(s)$ and a second order filter $H_2(s)$.

$$H_3(s) = H_1(s)H_2(s) \tag{2.26}$$

$$H_1(s) = \frac{\omega_0}{s+\omega_0} \tag{2.27}$$

$$H_2(s) = \frac{\omega_0^2}{s^2+2\xi\omega_0 s+\omega_0^2} \tag{2.28}$$

$$\omega_0 = \frac{2\pi f_m}{1.2}, \xi = 0.175$$

The analog filter is converted to the equivalent discrete time third order IIR filter using the bilinear transform. This method is simple to implement and as the filter produces one output at a time memory requirements are very less. In contrast the IDFT method [9] requires the entire sequence to be generated in one shot and stored in memory. This quickly becomes impractical for long simulation runs. The sequence that is output is a random sequence unlike the output of a the Jakes' Sum of Sinusoids [10] method which produces deterministic sequences. This is necessary because for the frequency selective fading model we need to generate the sequences for each tap and make sure they are uncorrelated.

CHAPTER III

EXPONENTIAL EFFECTIVE SNR MAPPING

In this chapter we present the Exponential Effective SNR Mapping (EESM) function which converts a multi-state channel into an equivalent single-state channel. A multi-state channel is one in which different sections of the codeword are received with different Signal to Noise Ratios(SNR) as opposed to a single-state channel where the entire codeword is received with a uniform SNR.

A. Basic Principle

When an OFDM symbol with N subcarriers is transmitted over a frequency selective channel each subcarrier has a different gain coefficient λ_k and consequently each subcarrier is received with a different SNR. The subcarrier coefficient is related to the channel tap coefficient realization through the Discrete Fourier Transform as

$$\lambda_k = \sum_{i=0}^{L-1} h_i e^{\frac{-j2\pi ki}{N}} \qquad k = 0, 1 \ldots N-1 \tag{3.1}$$

The instantaneous channel realization is therefore given by a set of SNR values $\bar{\gamma} = [\gamma_1, \gamma_2 \ldots \gamma_N]$ unlike the case of a flat fading channel where the channel realization is given by a scalar SNR. The EESM function introduced in [11] and [12] is a mapping function which can convert this set of SNR values into an equivalent scalar SNR γ_{EESM} that characterizes the channel condition. This equivalent SNR can be used to estimate the Block Error Ratio (BLER) for the realization by reading off the BLER corresponding to γ_{EESM} from the AWGN performance curves.

From the above discussion it is evident that the EESM is basically a mapping

function that satisfies the following equivalence.

$$BLER([\gamma_1, \gamma_2 \ldots \gamma_N]) \approx BLER_{AWGN}(\gamma_{EESM}) \tag{3.2}$$

B. Derivation for BPSK

The EESM function for the binary signaling case is derived in [11] based on the Union-Chernoff bound on error probabilities. The union bound for coded binary transmission and maximum-likelihood decoding given by

$$P_e(\gamma) \leq \sum_{d=d_{min}}^{\infty} \alpha_d P_2(d, \gamma) \tag{3.3}$$

where γ is the SNR, d_{min} is the minimum distance of the binary code, α_d is the number of codewords at a distance d and $P_2(d, \gamma)$ is the pairwise error probability for a given distance d at SNR γ.

For BPSK modulation the pair wise error probability can be upper bounded using the Chernoff bound as shown below

$$\begin{aligned} P_2(d, \gamma) &= Q(\sqrt{s\gamma d}) \\ &\leq e^{-\gamma d} \\ &= P_{2,Chernoff}(d, \gamma) \\ &= [P_{2,Chernoff}(1, \gamma)]^d \end{aligned} \tag{3.4}$$

From the union bound in the Probability of error can be expressed in terms of the Chernoff bounded pair-wise error probability as

$$\begin{aligned} P_e(\gamma) &\leq \sum_{d=d_{min}}^{\infty} \alpha_d P_2(d, \gamma) \\ &\leq \sum_{d=d_{min}}^{\infty} \alpha_d [P_{2,Chernoff}(1, \gamma)]^d \end{aligned}$$

$$= \quad P_{e,Chernoff}(\gamma) \tag{3.5}$$

When the channel no longer has a uniform SNR but has two states SNR in each being γ_1 and γ_2 and occurring with probability p_1 and p_2 respectively, the pair-wise error probability between two codewords at a Hamming distance can be expressed as

$$\begin{aligned} P_{2,Chernoff}(d,[\gamma_1,\gamma_2]) &= \sum_{i=0}^{d} dC_i p_1^i p_2^{d-i} e^{-(i\gamma_1+(d-i)\gamma_2)} \\ &= (p_1 e^{-\gamma_1} + p_2 e^{-\gamma_2}) \end{aligned} \tag{3.6}$$

Here the average pair-wise error probability over all distributions of the d differing symbols between the two states is considered. $(p_1 e^{-\gamma_1} + p_2 e^{-\gamma_2})$ is the averaged Chernoff-bounded symbol error probability for the two state channel. Thus the relationship between the Chernoff-bounded uncoded symbol error probability and the pair-wise error probability for the two state channel mirrors the relationship in the single state channel

$$P_{2,Chernoff}(d,[\gamma_1,\gamma_2]) = [P_{2,Chernoff}(1,[\gamma_1,\gamma_2])]^d \tag{3.7}$$

The above relation can be extended for the general multi-state channel characterized by $\bar{\gamma} = [\gamma_1, \gamma_2 \ldots \gamma_N]$ as

$$P_{2,Chernoff}(d,\bar{\gamma}) = [P_{2,Chernoff}(1,\bar{\gamma})]^d \tag{3.8}$$

The above properties of the Chernoff bounded error probabilities can be used to find the equivalent scalar SNR for a multi state channel realization. We need to find an equivalent SNR γ_{EESM} such that

$$P_{e,Chernoff}(\gamma_{EESM}) = P_{e,Chernoff}(\bar{\gamma}) \tag{3.9}$$

Using equations this is equivalent to

$$P_{2,Chernoff}(1, \gamma_{EESM}) = P_{2,Chernoff}(1, \bar{\gamma}) \tag{3.10}$$

which implies that

$$\gamma_{EESM} = -\ln(\sum_{k=1}^{N} p_k e^{-\gamma_k}) \tag{3.11}$$

For the OFDM case which has N subcarriers with different SNR values the equivalent SNR expressions becomes

$$\gamma_{EESM} = -\ln(\frac{1}{N}\sum_{k=1}^{N} e^{-\gamma_k}) \tag{3.12}$$

C. Extension to Other Modulation Schemes

The equivalent SNR for QPSK modulation can be derived in the same way and results in

$$\gamma_{EESM} = -\frac{1}{2}\ln(\frac{1}{N}\sum_{k=1}^{N} e^{-\frac{\gamma_k}{2}}) \tag{3.13}$$

It is more difficult to derive the EESM for other modulation schemes however the expressions for BPSK and QPSK show that the general form of the expression for other modulations is

$$\gamma_{EESM} = -\frac{1}{\beta}\ln(\frac{1}{N}\sum_{k=1}^{N} e^{-\frac{\gamma_k}{\beta}}) \tag{3.14}$$

where β is a parameter dependent on the specific modulation coding scheme and can be determined by simulation.

D. Calibration of β

The β parameter in the EESM function is determined through simulation for the higher order modulation schemes. A large number of realizations of the fading channel

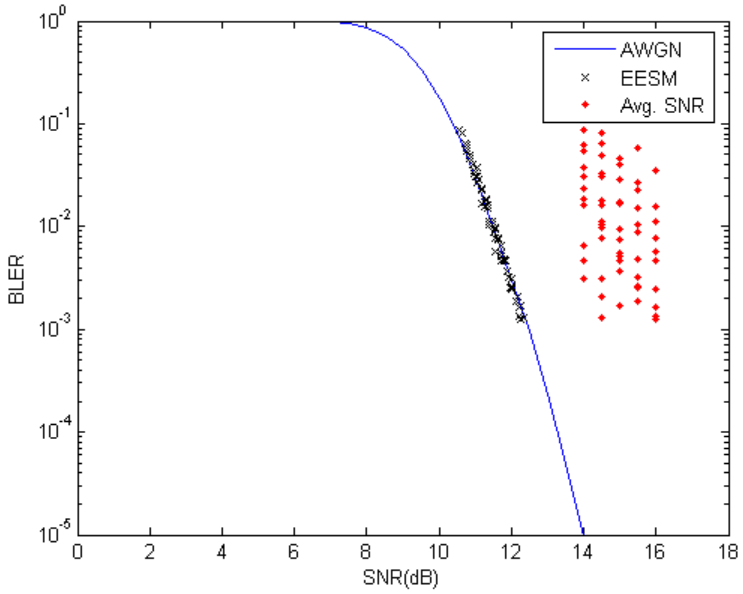

Fig. 6. Beta Calibration for 16QAM Rate 3/4

are generated. A realization for the frequency selective channel with OFDM is a set of SNR values with one SNR value per subcarrier. For each realization the actual BLER is determined by simulation. From the AWGN Block Error Rate curve we can get the SNR that corresponds to this BLER. This is the equivalent SNR of the frequency selective fading channel and this is the value that the EESM function should return. Therefore the optimum β value (3.15) is that value of β which minimizes the mean square error between the SNR corresponding to the actual BLER (from the AWGN curve) and the Effective SNR γ_{EESM} predicted by the EESM function. The minimization is done with the SNR in dB scale [13].

$$\beta_{opt} = \arg\min_{\beta} \mid SNR_{AWGN} - \gamma_{EESM}(\beta) \mid^2 \tag{3.15}$$

Some results for the β calibration are shown in Figs. 6 to 9. In Fig. 6 and Fig. 8 the ability of the EESM function to accurately map the SNR vector corresponding to

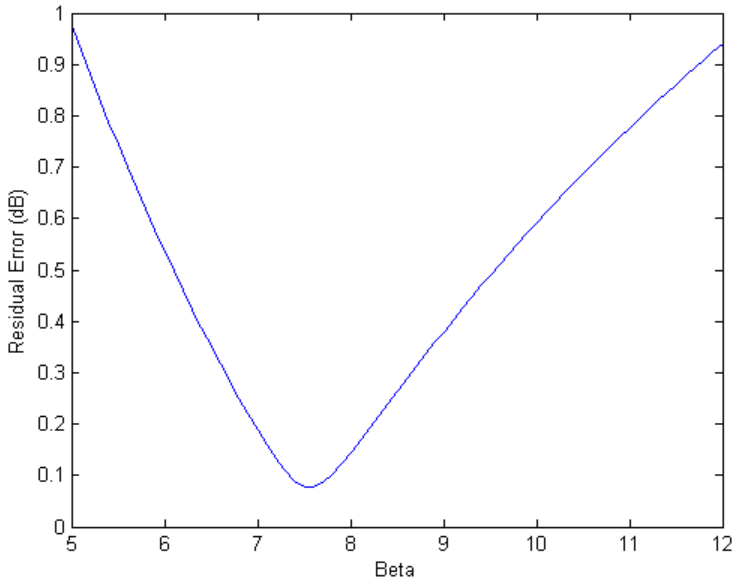

Fig. 7. Residual Error for 16QAM Rate 3/4

a realization to the equivalent AWGN SNR that produces the same BLER. On these each graphs each realization of the channel in β calibration produces a pair of points denoted by a red dot and a black x. These points share the same ordinate and that is the actual BLER for that realization determined by simulation. The abscissa of the red dot corresponds to the average of the realization SNR vector values and the abscissa of the black x is the equivalent SNR estimated by the EESM function with optimized β value. The black x's all line up on the AWGN BLER curve indicating that the EESM function has determined the scalar equivalent SNR that produces the same SNR. Figs. 7 and 9 show the residual error of the EESM mapping function for a range of β values. From the figures the optimum β value for 16QAM Modulation with rate 3/4 convolutional code is seen to be 7.6 and for 64QAM Modulation with rate 3/4 convolutional code it is 24.2.

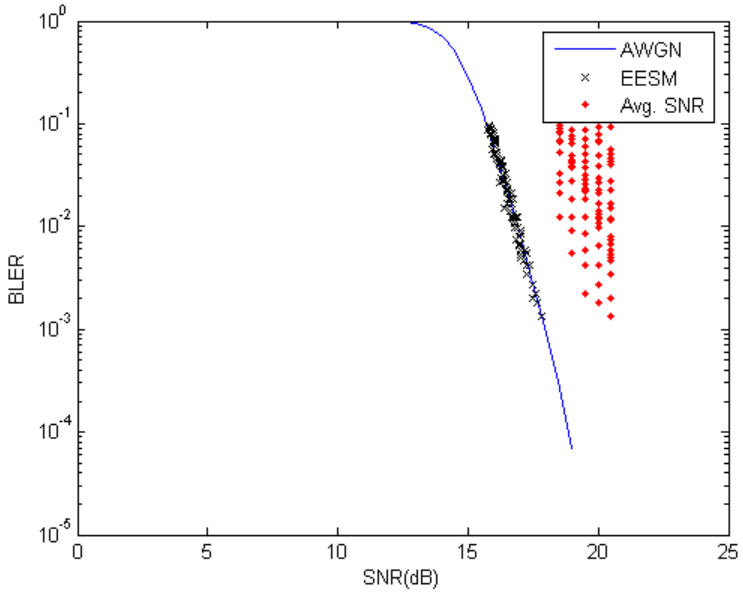

Fig. 8. Beta Calibration for 64QAM Rate 3/4

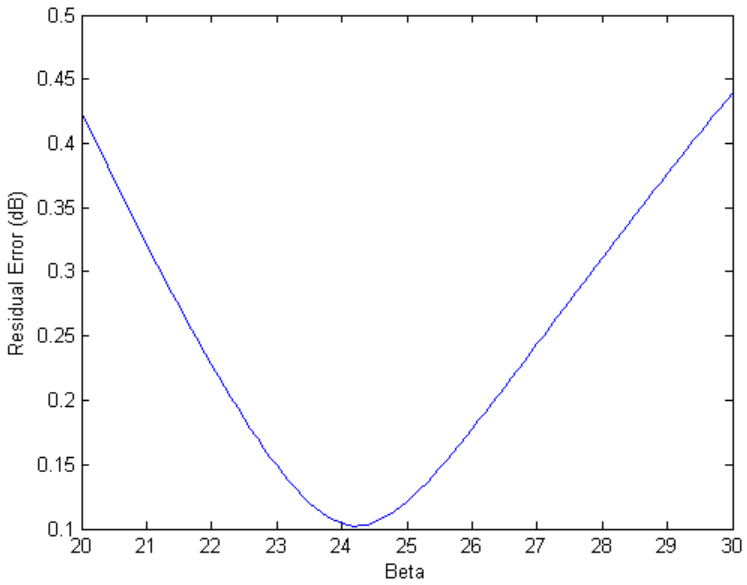

Fig. 9. Residual Error for 64QAM Rate 3/4

Table I. Optimized Beta Values and Residual Errors

MCS	Opt. Beta	Residual Error (dB)
QPSK 1/2	1.9	0.0386
QPSK 3/4	1.9	0.0751
16QAM 1/2	4.7	0.1197
16QAM 3/4	7.6	0.0762
64QAM 1/2	12.1	0.1939
64QAM 2/3	17.6	0.1461
64QAM 3/4	24.2	0.1022

Table. I contains the optimum β values for different modulation coding schemes and their residual errors.

CHAPTER IV

PHYSICAL LAYER MODELS

The most accurate method of conducting a network simulation involving wireless links would be to explicitly model the physical layer. This involves making each packet go through coding and modulation followed by passing the physical layer frames through an equivalent channel with appropriate fading and noise parameters and finally performing demodulation and decoding on the received packet to determine if it gets through error free. Though this sort of simulation might be the most accurate for assessing the impact of the physical layer on the network protocols, the running time makes it impossible to use in practice for even the simplest of network topologies. However it serves as the benchmark to compare other simpler models of the physical layer. In the following sections we examine some of the existing practically viable results on modeling the physical layer and their relative merits and demerits.

A. Two State Markov Model

The Two State Markov Model (2SMM) also known as the Gilbert-Elliott model [14] is the simplest and most widely widely model for the wireless link physical layer. The model shown in Figure 10 has two states - a good state and a bad state. The model is parameterized by the transition probabilities between the two states. Whenever the model is in the good state all the packets get through without error. Whenever the model is in the bad state all packets are dropped.

The parameters p and q are calculated from the Frame Error Rate (FER) and the Average Burst Error Length (ABEL). The relation between the parameters of the

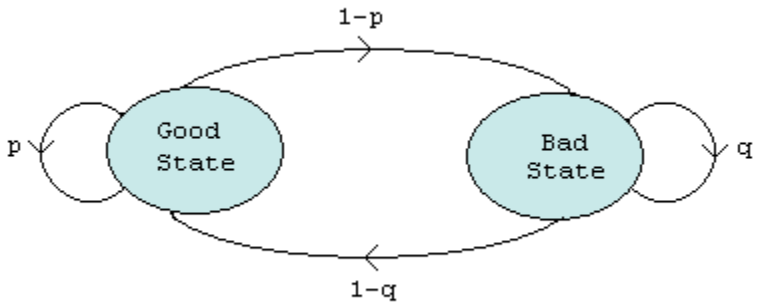

Fig. 10. Two State Markov Model

model p,q and the FER and $ABEL$ is shown below.

$$FER = \frac{1}{1-q} \tag{4.1}$$

$$ABEL = \frac{1-p}{2-p-q} \tag{4.2}$$

The FER and ABEL need to be determined by explicit simulation of the physical layer. From results presented in it is seen that the 2SMM is not a very accurate model for the wireless fading channel. It is shown that it underestimates the throughput for low to medium SNRs. However the 2SMM model despite its known drawbacks is still widely used due to its simplicity.

B. Finite State Markov Model

In this approach originally proposed by Wang in [15] the channel is divided into a number of states. The structure of the Finite State Markov Model (FSMM) is shown in Figure 11. Each state corresponds to a range of instantaneous SNR values. Transitions are only possible to the same state or adjacent states. As a state corresponds to a range of instantaneous SNR values the Frame Error Rate when the model is

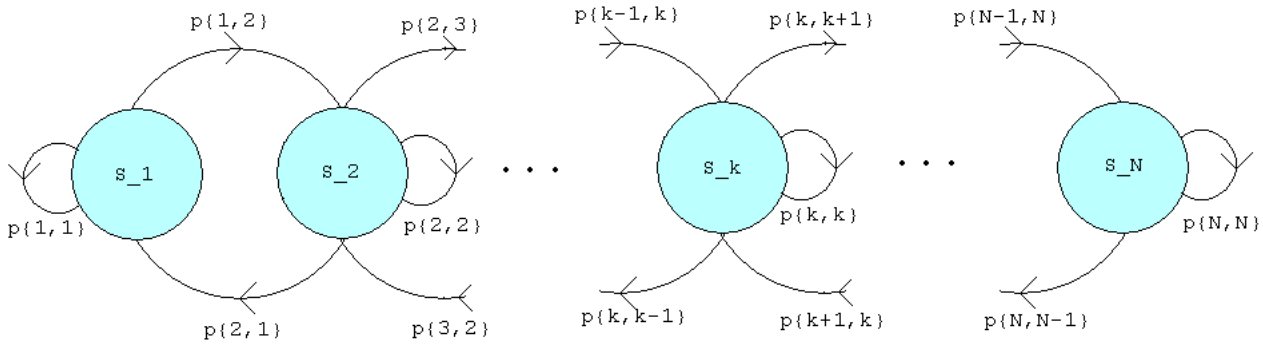

Fig. 11. Finite State Markov Model

in a particular state is given by the expectation of the FER over the range. The division of the instantaneous SNR into the states is done such that the average time that the fading process spends in each state is the same. The model is thus defined by the FER in each state and the transition probabilities between the states. These transition probabilities can be determined analytically using the level crossing rates at the SNR values separating the states.

The FSMM approach provides better results than the 2SMM but is a lot more complex. The FSMM performs better when the number of states is higher but this increases the number of parameters that need to be set up. Also the number of states that are needed to get good results can only be determined by trial and error. The number of states needed depends on the Doppler rate of the channel with more states being required for slower fading. Some alternate approaches to set up the FSMM are partitioning the instantaneous SNR such that all states are equiprobable or partitioning based on the the thresholds for an optimum Minimum Mean Square Error Lloyd-Max Quantizer for the SNR range. A generalized FSMC has been proposed in [16] where the limitation that the states can transition only to adjacent states is removed. This makes the model more flexible and enables setting up of the model

through simulation rather than the analytical transition probabilities alone.

The FSMM has been shown to provide better results than the 2SMM. However the large number of parameters that need to be determined and the complexity in setting it up have hindered widespread adoption of the model in practice.

C. Four State Markov Model

The Four State Markov Model (4SMM) has been proposed in [4] by Yu and simultaneously achieves the requirements of being a simple model and matching the true behavior of the physical layer. It is shown that matching the run length distributions of the good and bad frames produces results that agree closely with full physical layer simulations. Hence any model that accurately matches the good and bad frame run length distribution produced by the channel should perform reasonably well.

This model improves on the Two State Markov model by bifurcating both the good and bad states into two separate states each - one corresponding to long runs and the other to short runs. This is done guided by the observation that the run length distributions obtained from physical layer simulations look like a mixture of two different exponential slopes. Having a single good or bad state can only match one slope and hence does not perform as well as the 4SMM model which is able to match both portions. The 4SMM model attempts to match the slopes at both ends of the run length distribution curve (short runs and long runs) by using a mix of geometric distributions. The run length distribution of the 4SMM model illustrated in Figure 12 is given by $f(k)$

$$f(k) = p(1-a)a^k + (1-p)(1-b)b^k \tag{4.3}$$

The parameters of the model are a the initial slope of the run length distribution,

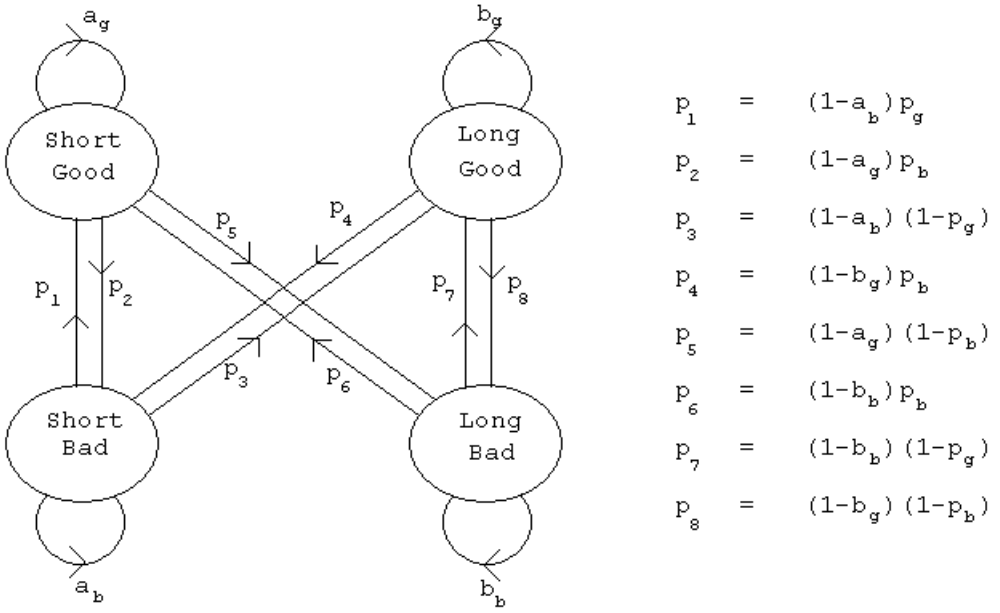

Fig. 12. Four State Markov Model

b the tail slope of the run length distribution and the p the fraction of short runs or the mixing probability. Therefore the 4SMM is completely characterized by two sets of parameters - $\{a_g, b_g, p_g\}$ for the good run length distribution and $\{a_b, b_b, p_b\}$ for the bad run length distributions.

The 4SMM model is relatively easy to set up and also is simple to execute in a simulation. For the flat Rayleigh fading channel an entirely analytical approach to setting up the model is presented. This coupled with the fact that the simulation results match the full physical layer model very closely make it an excellent model for the physical layer in a wireless channel simulation.

D. 4SMM Parameters

We omit the detailed derivations of the formulae found in [4] for setting up the 4SMM and present the key results that are used to set up the parameters of the 4SMM to match the run length distributions.

1. Tail Exponential Slope

The tail of the run length distributions corresponds to long bursts of frames received in error for the bad frame run lengths. This is caused when the instantaneous SNR drops below a threshold γ_l and all the frames are received in error. Therefore having to determine the tail exponential slope for the bad runs is equivalent to finding the tail slope of the distribution of the time duration which the fading process spends below the threshold γ_l. Similarly it can be reasoned that good frame runs are caused when the instantaneous SNR remains above a threshold γ_u and the tail exponential slope for the good runs can be obtained from the distribution of the time duration that the fading process spends above γ_u. The thresholds γ_l and γ_r are chosen as the points Frame Error Rate curve of the particular modulation coding scheme in AWGN where the Frame Error Rate is greater than 99% and less than 1% respectively. The b_b and b_g values corresponding to the tail slopes of the bad frame and good frame run length distributions respectively can thus be calculated from the cumulative distribution function of the instantaneous SNR as

$$b_b = (Pr[\gamma < \gamma_l])^{T_f/\Delta_t} \tag{4.4}$$

$$b_g = (Pr[\gamma > \gamma_u])^{T_f/\Delta_t} \tag{4.5}$$

T_f is the frame duration and Δ_t is the smallest value for which the channel decorrelates. Δ_t is set to $\frac{1.2}{\pi f_m}$

2. Initial Exponential Slope

The initial slope of the run length distributions correspond to short runs of good and bad frames interspersed with one another. These are caused when the instantaneous SNR is between the thresholds γ_l and γ_u. It is argued and also confirmed by experimental results that the short runs are independent of the Doppler rate, long term average SNR and the specifics of the modulation, coding or frame sizes of the physical layer. Therefore the values are a_g and a_b are set to 0.5 and are seen to adequately match the initial exponential slopes of the run lengths.

3. Combination Factor

The combination factor p denotes the fraction of short runs in the total number of runs. The mixing probabilities are calculated in terms of the ratio of the number of short and long run lengths per second.

$$p = \frac{N_s}{N_s + N_l} \tag{4.6}$$

where N_s and N_l are the number of short and long runs per second respectively.

Everytime the instantaneous SNR of the fading process crosses γ_u in the upward direction it causes a long run of good frames because all frames are received correctly in this SNR range. Similarly when the SNR crosses γ_l in the downward direction it causes a long run of bad frames. Therefore the number of long runs per second N_l for the good runs and the bad runs is equal to the level crossing rate of the fading process at γ_u and γ_l respectively.

The number of short runs per second can be determined from the AWGN Frame Error rate curve and the distribution of the instantaneous SNR

$$N_s = \int_{\gamma_l}^{\gamma_u} P(\gamma) P_e(\gamma)(1 - P_e(\gamma)) d\gamma \tag{4.7}$$

where $P(\gamma)$ is the probability density function (pdf) of the instantaneous SNR and $P_e(\gamma)$ is the probability of Frame Error at SNR γ.

The combination factors p_g and p_b can also be setting up using average run length obtained from the good and bad frame error distributions τ_g and τ_b respectively. For the 4SMM generated frame error process the average run length is given by

$$\tau = \frac{p}{1-a} + \frac{1-p}{1-b} \tag{4.8}$$

The p parameters can be chosen such that it matches the actual good and bad average frame lengths obtained from simulation.

$$p = \frac{\tau - \frac{1}{1-b}}{\frac{1}{1-a} - \frac{1}{1-b}} \tag{4.9}$$

From the above expressions we see that the 4SMM can be completely set up using

- PDF of the instantaneous SNR of the fading process
- Level Crossing Rate of instantaneous SNR at the thresholds γ_l and γ_u
- Frame Error Probability as a function of SNR

E. EESM Alternative for Setting Up 4SMM

For the flat Rayleigh fading case analytical expressions for the PDF of the instantaneous SNR and the level crossing rates are well known and the model parameters can be readily calculated. For the frequency selective case also analytical expressions have been developed. However when setting up the 4SMM Markov model the diversity order achieved by the particular modulation coding scheme at the SNR of interest is required. The maximum achievable diversity order is limited by the minimum of the

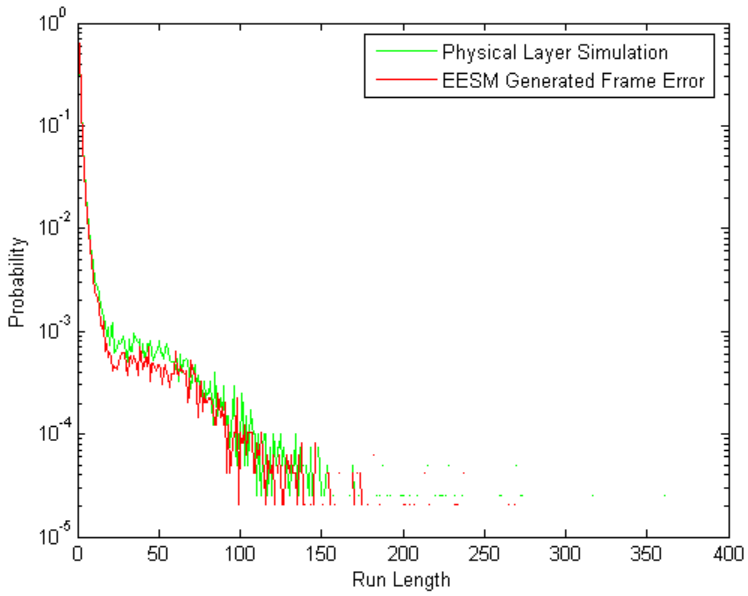

Fig. 13. Bad Frame Run Length Distributions at 6dB

diversity available in the channel (the number of paths L) and the minimum distance of the codeword. However this is only an asymptotic limit and the diversity order that is actually achieved is a function of the SNR and could lie anywhere between 1 and the maximum. This value has to be obtained by a full simulation of the specific physical layer and the channel. It also needs to be recalculated at different SNRs.

This problem arises due to the fact that the channel is frequency selective but we have demonstrated in the previous chapter that the EESM function is able to convert a frequency selective fading process into an equivalent flat fading process. In Figures 13 to 16 the frame error run length distributions obtained by a full physical layer simulation are compared with distributions obtained using the EESM function. For the EESM distributions long runs (approx. 1 million samples) of frequency selective channel realizations with the appropriate correlation were generated. The EESM function was used to map the vector of SNR values for each realization into the

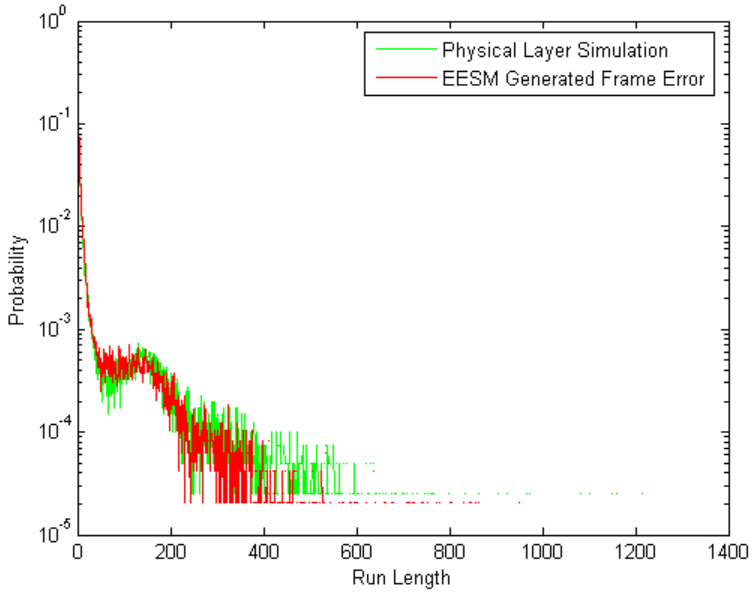

Fig. 14. Good Frame Run Length Distributions at 6dB

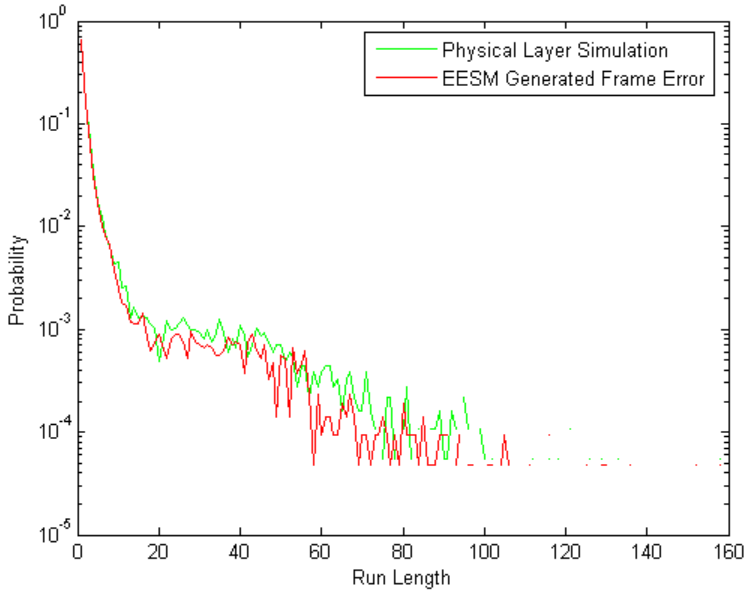

Fig. 15. Bad Frame Run Length Distributions at 8dB

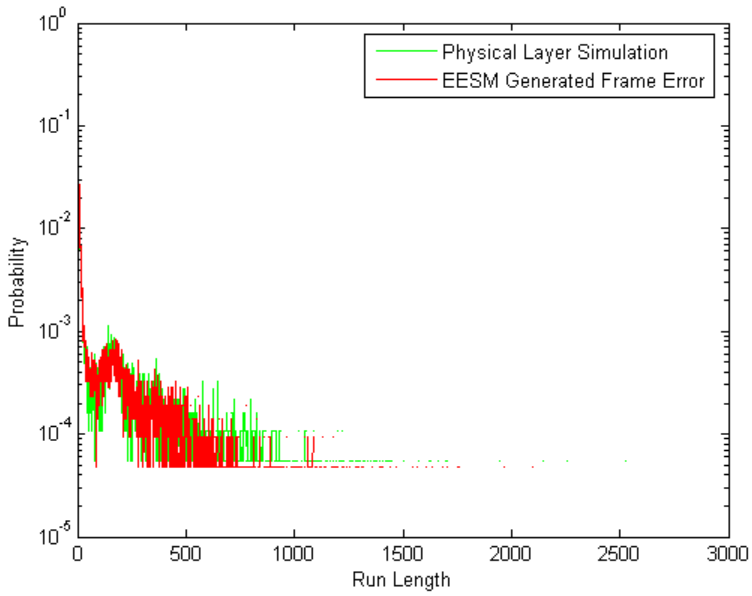

Fig. 16. Good Frame Run Length Distributions at 8dB

equivalent scalar SNR. The Frame Error Rate corresponding to this SNR was obtained from the AWGN FER curve and the frame was dropped with this probability. The resulting frame error pattern gives the good and bad frame run length distributions. The EESM generated distribution matches the true run length distribution of the channel very closely. This is encouraging as we know that matching the run lengths is the key to an accurate model. Hence it should be possible to set up the 4SMM model for a frequency selective channel using the EESM equivalent fading process without having to evaluate the diversity order.

F. 4SMM Model Parameters Using EESM

The Exponential Effective SNR Mapping as defined in the previous chapter converts the frequency selective fading channel into an equivalent flat fading channel with

instantaneous SNR γ_{EESM}.

$$\gamma_{EESM} = -\beta \log \left(\frac{1}{N} \sum_{i=1}^{N} \exp^{\frac{-\gamma_i}{\beta}} \right) \tag{4.10}$$

where β is an experimentally determined parameter that depends on the modulation coding schemes used and γ_i's are the SNR per subcarrier. When the number of independent taps in the multipath channel is less than N the correlation between the γ_i's is nonzero. In other words the term inside the log which is the mean of N correlated terms behaves approximately as the mean of L independent terms. Therefore the equivalent SNR can be approximated as

$$\begin{aligned} \gamma_{EESM} &\approx -\beta \log \left(\frac{1}{L} \sum_{k=1}^{L} \exp^{\frac{-\gamma_k}{\beta}} \right) \\ &= -\beta \log \left(\frac{1}{L} \sum_{k=1}^{L} R_k \right) \\ &= -\beta \log (R) \end{aligned} \tag{4.11}$$

To set up the 4SMM in terms of the EESM function we need to characterize the probability density function and the level crossing rate of the equivalent fading process. We also need to characterize the Frame Error Probability in terms of the equivalent SNR. From 4.11 we see that $R = \exp^{\frac{-\gamma_{EESM}}{\beta}}$ and as it is just a simple transformation of γ_{EESM} we can set up the 4SMM parameters in terms of R as it is more convenient.

1. Probability Density Function

$R = \frac{1}{L} \sum_{k=1}^{L} R_k$ is the sum of L iid variables R_i. Each R_i is the negative exponential of a Rayleigh distribution with power equal to the Average SNR of the channel and scaled by the EESM β parameter. It can be shown that pdf of R_i is nonzero between 0 and 1 and the exact distribution is determined by the ratio of Average SNR to the

β parameter.

$$P_{R_i}(x) = \frac{1}{\alpha} x^{\frac{1}{\alpha}-1} \quad 0 < x < 1 \tag{4.12}$$

where $\alpha = \bar{\gamma}/\beta$ with $\bar{\gamma}$ being the Average SNR of the channel.

As R is the sum of L independent variables its pdf is the L-fold convolution of the pdf of each individual R_i

$$P_R(x) = \frac{1}{\alpha^L} \left(x^{\frac{1}{\alpha}-1} * ... * x^{\frac{1}{\alpha}-1} \right) \tag{4.13}$$

For integer values of $\frac{1}{\alpha}$ the pdf can be obtained analytically. For other values the pdf can be obtained through numerical integration or by curve fitting to the experimentally obtained pdf.

2. Level Crossing Rate

The Level Crossing Rate of γ_{EESM} needs to be determined at the SNR thresholds or equivalently the level crossing rates of R at levels $r_1 = \exp^{\frac{-\gamma_l}{\beta}}$ and $r_2 = \exp^{\frac{-\gamma_u}{\beta}}$.

The level crossing rate of R can be calculated as

$$\begin{aligned}
L(R) &= P(R) \int_0^\infty \dot{R} P(\dot{R}|R)\, d\dot{R} \\
&= \int_0^\infty \dot{R} P(\dot{R}, R)\, d\dot{R} \\
&= \int_0^\infty \int_0^1 ... \int_0^1 \dot{R} P(\dot{R}, R, R_1, ..., R_L)\, dR_1 ... dR_L d\dot{R} \\
&= \int_0^\infty \int_0^1 ... \int_0^1 \dot{R} P(\dot{R}|R, R_1, ..., R_L) P(R|R_1, ..., R_L) P(R_1, ..., R_L)\, dR_1 ... dR_L d\dot{R} \\
&= \int .. \int_{R_1..R_L : R = \frac{1}{L}\sum_{k=1}^{L} R_k} P(R_1, ..., R_L) \int_0^\infty \dot{R} P(\dot{R}|R_1, ..., R_L)\, d\dot{R}\, dR_1 ... dR_L
\end{aligned} \tag{4.14}$$

As the R_k's are independent we get

$$\begin{aligned} P(\dot{R}|R_1,...,R_L) &= P\left(\left(\frac{1}{L}\sum_{k=1}^{L}\dot{R}_k\right)|R_1,...R_L\right) \\ &= P\left(\frac{1}{L}\sum_{k=1}^{L}\dot{R}_k|R_k\right) \end{aligned} \tag{4.15}$$

For a unit power Rayleigh flat fading process with envelope r it is known that

$$P(\dot{r}) \sim N(0,\sigma_v^2) \tag{4.16}$$

where $\sigma_v^2 = (\pi f m)^2$ with f_m the maximum Doppler shift [17].

$$R_k = \exp^{-\alpha r^2} \tag{4.17}$$

$$\dot{R}_k = -2\alpha r\dot{r}\exp^{-\alpha r^2} \tag{4.18}$$

Therefore,

$$P(\dot{R}_k|R_k) \sim N(0, 4\sigma_v^2\alpha R_k^2\log(R_k^{-1})) \tag{4.19}$$

and as a consequence of the R_k's being independent

$$P(\dot{R}|R_1..R_L) \sim N(0, \frac{4}{L^2}\sigma_v^2\alpha\sum_{k=1}^{L}R_k^2\log(R_k^{-1})) \tag{4.20}$$

Using the above results we can write

$$\begin{aligned} L(R) &= \int..\int_{R_1..R_L:R=\frac{1}{L}\sum_{k=1}^{L}R_k} P(R_1,...,R_L)\int_0^\infty \dot{R}P(\dot{R}|R_1,...,R_L)\,d\dot{R}\,dR_1...dR_L \\ &= \frac{1}{\alpha^L}\int..\int_{R_1..R_L:R=\frac{1}{L}\sum_{k=1}^{L}R_k}\prod_{k=1}^{L}R_k^{\frac{1}{\alpha}-1}\int_0^\infty \dot{R}P(\dot{R}|R_1,...,R_L)\,d\dot{R}\,dR_1...dR_L \\ &= \frac{\sqrt{2\pi\alpha}f_m}{L\alpha^L}\int..\int_{R_1..R_L:R=\frac{1}{L}\sum_{k=1}^{L}R_k}\prod_{k=1}^{L}R_k^{\frac{1}{\alpha}-1}\sqrt{\sum_{k=1}^{L}R_k^2\log(R_k^{-1})}\,dR_1...dR_L \end{aligned} \tag{4.21}$$

The level crossing rate can be calculated from the above integral at the thresholds

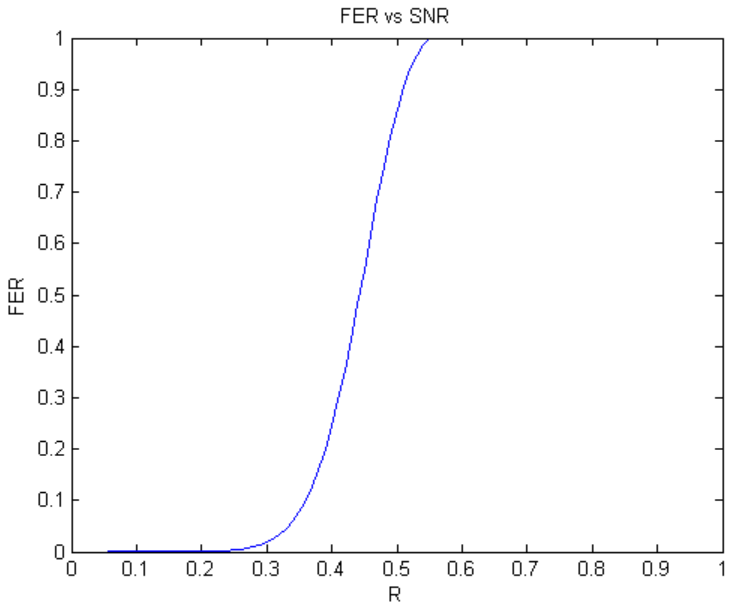

Fig. 17. Frame Error Rate in Terms of R

$R = r_1$ and $R = r_2$

3. Frame Error Probability

The frame error probability is obtained for the AWGN channel by simulation. As the pdf and level crossing rates of the equivalent fading process are derived in terms of R it is easier to perform the calculation of the 4SMM parameters by converting the Frame Error Probability to a function of R.

Figure 17 shows the FER as a function of R. The relation between R and γ_{EESM} is $\gamma_{EESM} = -\beta \log(R)$ which implies that a low R value close to 0 corresponds to high SNR and an R value close to 1 corresponds to a low SNR.

G. Results

1. Physical Layer Description

The 4SMM model was set up using the EESM equivalent fading process and results compared with a physical layer simulation. The physical layer simulated was based on the IEE 802.11a standard for wireless LANs. The IEEE 802.11a standard uses a 64 subcarrier OFDM. Data is sent on 48 subcarriers and the other subcarriers are used for pilots and guard band purposes. The standard specifies a 16 symbol cyclic prefix. It provides a wide variety of rates from 6Mbps to 54 Mbps to be adaptively switched based on channel conditions. The results presented here are for the 12Mbps rate mode which employs QPSK modulation and the Forward Error Correction comprises of a Rate 1/2 terminated-trellis convolutional code with the standard generator polynomials $\{171_8, 133_8\}$.

The channel is a four tap frequency selective channel (L=4). Each tap is Rayleigh faded and the taps are uncorrelated and have equal power. The payload on each frame 378 data bits. Accounting for the 6 trellis termination bits gives 384 uncoded bits which are encoded, modulated and packed into a frame. The frame duration for this size at the 12Mbps rate is 32μs. The simulations are performed for a Doppler of 100Hz and 50Hz. The fading coefficients for the channel taps are generated by the third order filtering method described in Chapter II.

2. Run Length Distributions for 4SMM Using EESM

The run length distribution of the 4SMM model for the 4 tap channel is compared with the good and bad frame error distributions obtained from the physical layer simulation. Results are presented for Average SNR 6dB and 8dB at Doppler of 100Hz and 50Hz.

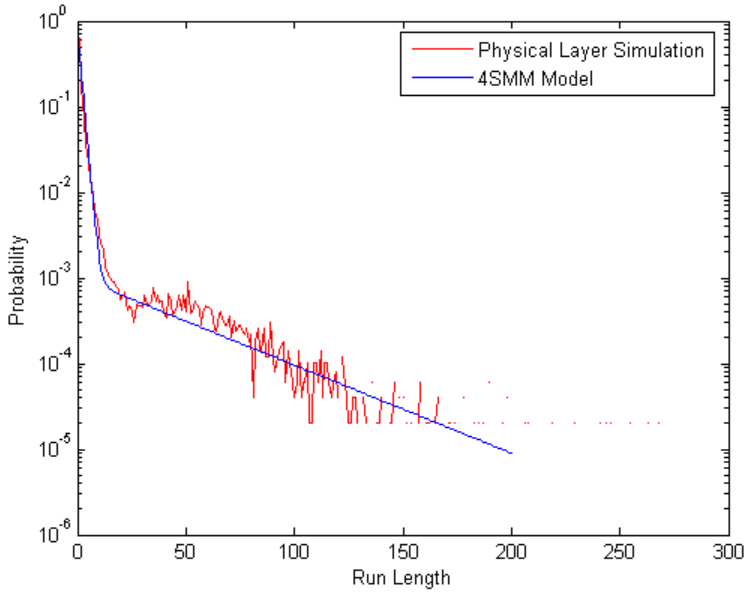

Fig. 18. Bad Frame Run Length Distributions at 6dB, Doppler 100Hz

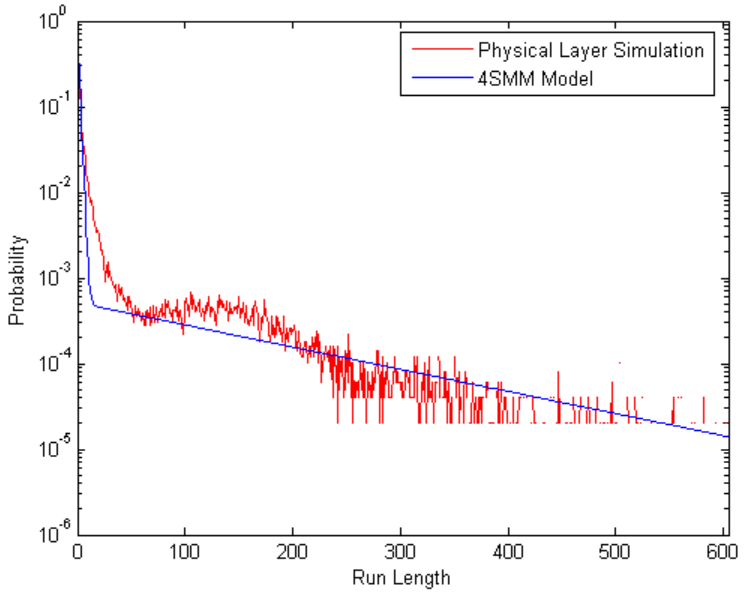

Fig. 19. Good Frame Run Length Distributions at 6dB, Doppler 100Hz

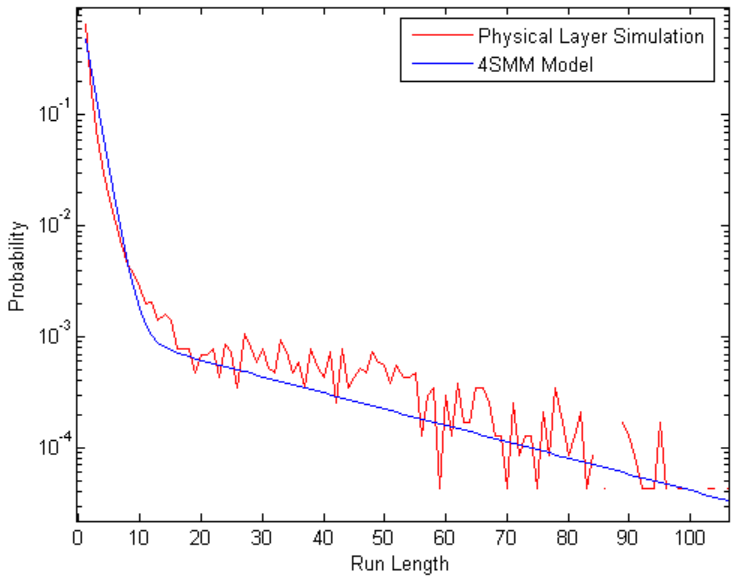

Fig. 20. Bad Frame Run Length Distributions at 8dB, Doppler 100Hz

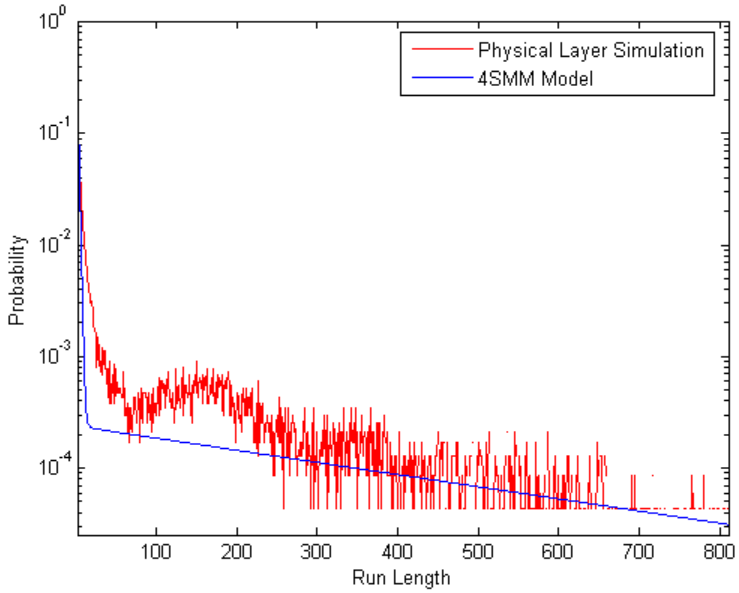

Fig. 21. Good Frame Run Length Distributions at 8dB, Doppler 100Hz

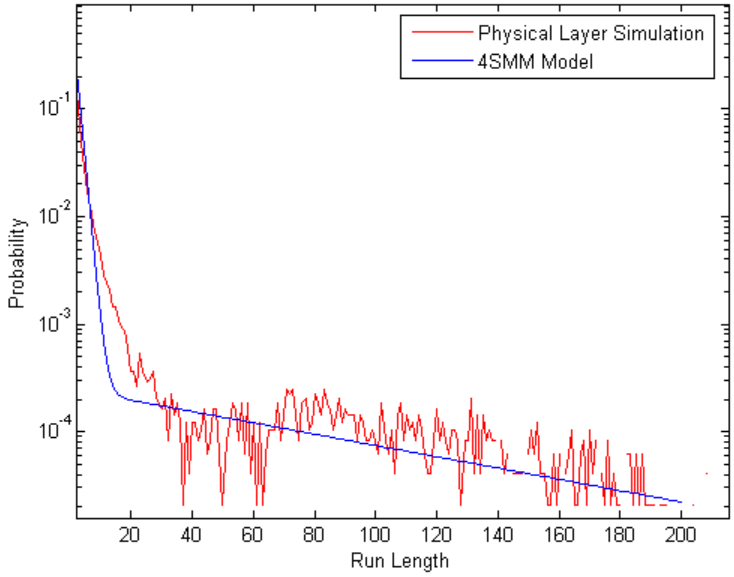

Fig. 22. Bad Frame Run Length Distributions at 6dB, Doppler 50Hz

Figures. 18 to 21 are the run lengths for the 100Hz channel and Figures. 22 to 25 are for the 50Hz channel. From the plots we can see that the 4SMM model set up using the EESM method models the run length properties of the frame errors induced by the physical channel very well. The model provides a good match for all the SNR and the Doppler cases studied.

3. Comparison with FSMM

The equivalent flat fading process generated by the EESM function can be employed to set up other models for the physical layer too. Here we study the performance of the Finite State Markov Model(FSMM) when using the EESM equivalent fading process to determine the transition probabilities for the FSMM. We use the generalized model that does not constrain transitions to occur only between states. The range of the instantaneous SNR is partitioned into 16 states.

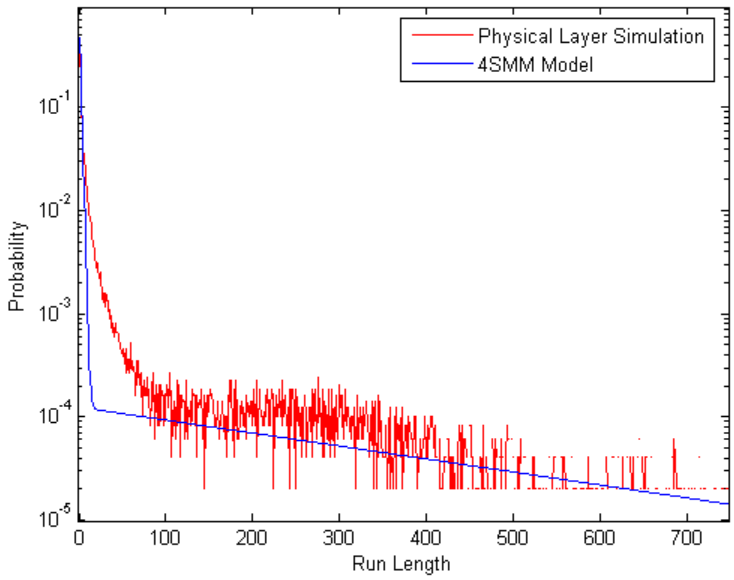

Fig. 23. Good Frame Run Length Distributions at 6dB, Doppler 50Hz

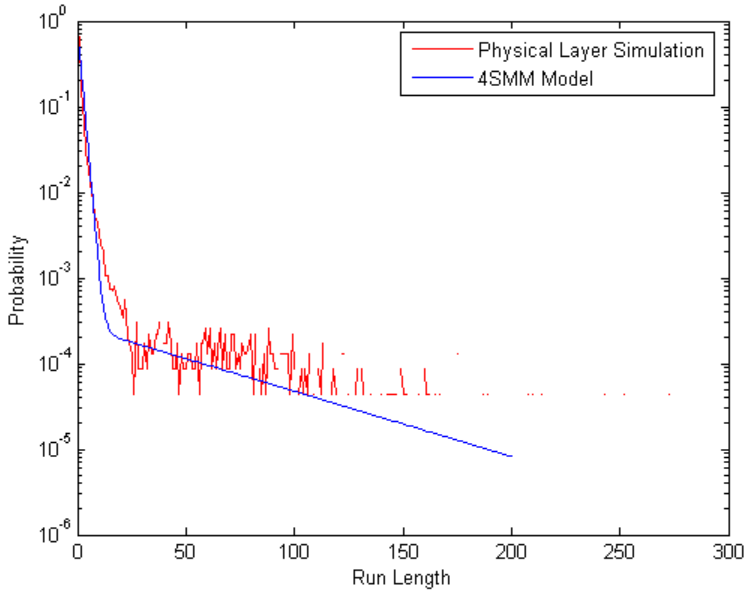

Fig. 24. Bad Frame Run Length Distributions at 8dB, Doppler 50Hz

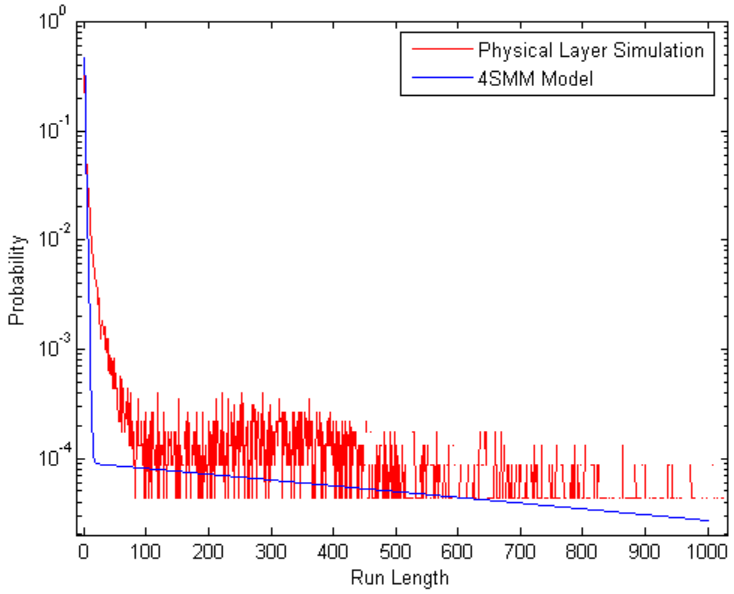

Fig. 25. Good Frame Run Length Distributions at 8dB, Doppler 50Hz

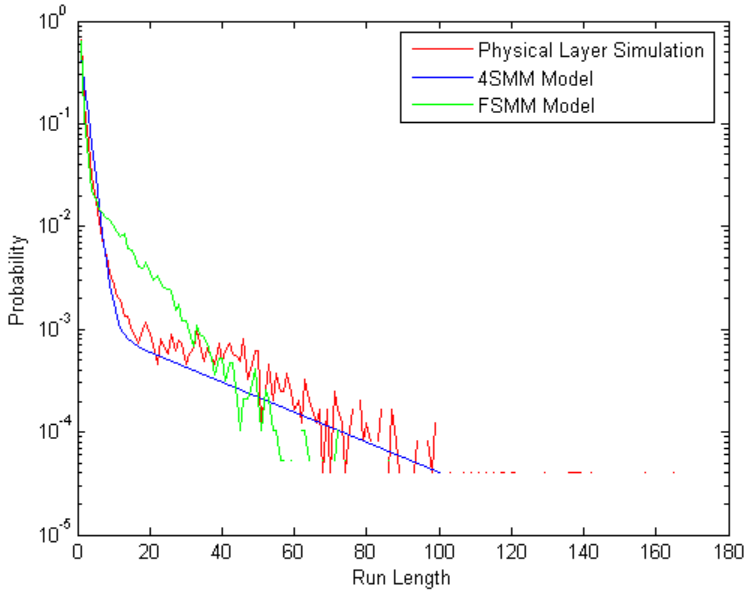

Fig. 26. FSMM vs FSMC Bad Frame Run Length Distributions at 8dB

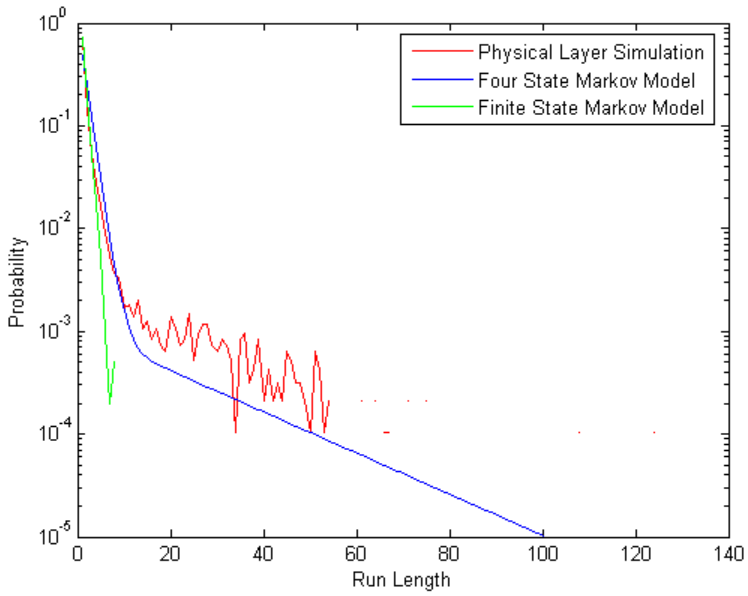

Fig. 27. FSMM vs FSMC Bad Frame Run Length Distributions at 10dB

Figures. 26 and 27 compare the performance of the Finite State Markov Model set up using EESM with the Four State Markov Model also set up with EESM. It is seen that the FSMM does not accurately capture the slope of the run length distribution as the 4SMM does. This is something expected as this is the case with flat fading case too where the 4SMM outperforms the FSMM in matching the run length distribution tail slope.

CHAPTER V

CONCLUSION

The physical layer models for wireless links in a network simulation were studied especially for the broadband channel with frequency selective fading. The use of the Effective Exponential SNR Mapping function for converting the frequency selective channel into an equivalent flat fading channel was explored. It was seen that the EESM function provides a good estimate of the Frame Error Rate of a frequency selective fading channel realization using the AWGN performance characteristics for the modulation and coding scheme. The β parameter for different modulation and coding schemes was determined.

Among the models proposed to model the effect of the physical layer in a fading environment the 4SMM model performs the best in terms of matching the frame error statistics of the fading process. The ability of the EESM function to convert a frequency selective realization determined by a vector of SNR values into a scalar SNR corresponding to an equivalent flat channel was employed to set up the 4SMM model. This makes it easier to set up for the frequency selective case as there is no longer the need to determine how much diversity gain the system achieves at a particular SNR value for the given channel. The analytical formulations for setting up the 4SMM require the probability density function and the level crossing rates of the fading process. The probability density function and the level crossing rate expressions for the EESM equivalent fading process were derived.

Finally the performance of the 4SMM model set up using the EESM function was compared with the results gathered from running a detailed physical layer on the frequency selective wireless channel. It has been shown that the key to getting an accurate portrayal of the effect of the channel in conjunction with the physical layer

on the higher layers is to have a good match between the run length distributions of the model generated frame error process and the actual error process produced by the channel. The results obtained show a close match between the EESM Four State Markov Model good and bad frame run length distributions and that produced by the channel. A comparison was made with the Finite State Markov Model also set up using the EESM equivalent flat fading process and the 4SMM gives better a match than the FSMM. This validates the use of the 4SMM model as a simpler and more accurate model for matching wireless channel behavior than other current existing models. In summary a method to set up the 4SMM model for a frequency selective channel using the EESM equivalent fading process was developed and good results in terms of matching the frame error process statistics of the wireless channel were obtained.

REFERENCES

[1] Intel, "Understanding Wi-Fi and WiMAX as metro access solutions," http://www.intel.com/netcomms/technologies/wimax/wimax_docs.htm, 2004.

[2] M. Progler, C. Evci, and M. Umehira, "Air interface access schemes for broadband mobile systems," *IEEE Communications Magazine*, vol. 37, no. 9, pp. 106 – 115, September 1999.

[3] V. Jacobson and M. J. Karels, "Congestion avoidance and control," in *SIGCOMM '88 Workshop*, 1988, pp. 314–329.

[4] Y. Yu, "Physical layer model design for wireless networks," Ph.D. dissertation, College Station, TX: Texas A&M University, August 2006.

[5] A. Goldsmith, *Wireless Communications*, New York, NY: Cambridge University Press, 2005.

[6] D. Tse and P. Viswanath, *Fundamentals of Wireless Communications*, New York, NY: Cambridge University Press, 2005.

[7] V. Ramaswamy, "A comparative study of Rayleigh fading wireless channel simulators," M.S. thesis, College Station, TX: Texas A&M University, December 2005.

[8] S. L. Miller, *ELEN 489 Class Notes*, College Station, TX: Department of Electrical Engineering, Texas A&M University, Spring 2005.

[9] D. J. Young and N. C. Beaulieu, "The generation of correlated Rayleigh random variates by Inverse Discrete Fourier Transform," *IEEE Transactions on Communications*, vol. 48, pp. 1114–1127, July 2000.

[10] W. C. Jakes, *Microwave Mobile Communication*, New York, NY: IEEE Press, 1993.

[11] Ericsson, "System-level evaluation of OFDM further considerations," Lisbon: 3GPP TSG-RAN WG1 #35, R1-031303, 2003.

[12] Nortel Networks, "Modelling of performance with coloured interference using the EESM," Montreal: 3GPP TSG-RAN WG1 #37, R1-040509, 2004.

[13] E. Westman, "Calibration and evaluation of the Exponential Effective SINR mapping (EESM) in 802.16," M.S. thesis, Stockholm: Royal Institute of Technology (KTH), September 2006.

[14] E. N. Gilbert, "Capacity of burst noise channels," *The Bell System Technical Journal*, vol. 39, pp. 1253–1256, 1960.

[15] H. S. Wang and N. Moayeri, "Finite-state Markov channel-a useful model for radio communication channels," *IEEE Trans. Veh. Technology*, vol. 44, pp. 163–171, February 1995.

[16] Y. L. Guan and L. F. Turner, "Generalised FSMC model for radio channels with correlated fading," *IEE Proceedings Communications*, vol. 146, no. 2, pp. 133–137, 1999.

[17] G. L. Stuber, *Principles of Mobile Communication*, Boston, MA: Kluwer Academic Publishers, 2001.

VITA

Rajkumar Samuel was born in 1982 in Madras, India. He received his B.E in Electronics and Communication from Anna University, India. He received the Master of Science degree in Electrical Engineering from Texas A&M University in May 2007. His permanent address is Department of Electrical Engineering, Texas A&M University, College Station, TX 77843.

The typist for this thesis was Rajkumar Samuel.